



## EFFECT OF HOT ROLLING AND SOLUTION TREATMENT ON THE MICROSTRUCTURE AND MECHANICAL PROPERTIES OF Fe-Mn-Si-Cr-Ni SHAPE MEMORY ALLOY

Miftakhur Rohmah<sup>a,\*</sup>, Emmanoela Carissa Sendouw<sup>b</sup>, Rifqi Aulia Tanjung<sup>b</sup>, Dedi Pria Utama<sup>a</sup>, Efendi Mabru<sup>a</sup>

<sup>a</sup>Research Center for Metallurgy, National Research and Innovation Agency  
B.J. Habibie Sains and Technology Area, Banten, Indonesia 15314

<sup>b</sup>Department of Materials and Metallurgical Engineering, Institut Teknologi Kalimantan  
Soekarno Hatta KM 15, Balikpapan, Kalimantan Timur, Indonesia, 76127

\*E-mail: [miftakhur.rohmah@brin.go.id](mailto:miftakhur.rohmah@brin.go.id)

Received: 14-03-2023, Revised: 17-07-2023, Accepted: 01-08-2023

### Abstract

*Fe-14Mn-4Si-8Ni-11Cr SMA (shape memory alloy) was designed as a smart material because of its specific properties, which can memorize the original shape, so it has the potential to dampen vibration in seismic structures. Memory effect is triggered by SIM (stress-induced martensitic) transformation from  $\gamma$ -austenite to  $\epsilon$ -martensite (hexagonal close-packed / HCP) structure, and it is recovered by heating after unloading. This study investigated the effect of hot rolling and solution treatment on the microstructure and its relationship with hardness and SME (shape memory effect) properties. The as cast of Fe-14Mn-4Si-8Ni-11Cr was hot rolled (900 and 1000 °C) and solution treated (1000 and 1100 °C). After the thermomechanical process, all microstructures consist of  $\gamma$ -FCC (face-centered cubic), the annealing twins, and a fine band of  $\epsilon$ -martensite. The grain size of the  $\gamma$ -phase is 29.43, 41.96, 42.44, and 45.57  $\mu\text{m}$  for samples B, C, D, and E, respectively. The higher the temperature of hot rolling and solution treatment applied, the larger the grain size obtained, indirectly reducing the hardness to 299.93 BHN and 286.52 BHN for samples D and E. The coarsened austenite grain, a lower number of annealing twins, and the pre-existing line band of  $\epsilon$ -martensite are favorable to obtain the enormous recovery strain, up to 8.26% for sample E.*

**Keywords:** Fe-Mn-Si-Ni-Cr, SMA (shape memory alloy), SME (shape memory effect), strain recovery

### 1. INTRODUCTION

Shape memory alloy is an intelligent material that can revert to its original form after deformation, which became critical for biomedical, construction, automotive, and aerospace applications. In terms of earthquake resistance construction, SMA (shape memory alloy) can dampen vibrations, reduce the destruction effect, and provide a seismic response by self-centering capabilities despite extensive deformation [1]-[2]. As a result of these desirable properties, SMA might be employed to improve the existing structures, such as beam-column connections, specific braces, pre-stressing bars,

dissipation dampers, and base isolation systems. In two decades, some researchers have been interested in the development of Fe-based SMAs due to their high mechanical properties (good workability and machinability), higher thermal hysteresis, lower production preparation costs, and relatively SME (shape memory effect) when compared to NiTi-based and Cu-based [1],[3]. When Fe-Mn-Si SMA alloy is heated or loaded, the heat or stress-induced martensitic transformation from  $\gamma$ -austenite (face-centered cubic/FCC) to  $\epsilon$ -martensite (hexagonal close-packed/HCP) structure and its reversion during cooling or unloaded [3]. The ability to transform reverse (FCC  $\leftrightarrow$  HCP) by generating the strain-

induced epsilon martensite ( $\epsilon$ -SIM) is the most appropriate indicator of SME levels.

The shape memory ability depends on the morphology and orientation of the parent phase (austenite) for its transformation site [4]. Unfortunately, the SME and recovery strain effect of polycrystalline Fe-Mn-Si was lower (2-4%) than that of single crystal (~9%) due to variations of orientation in polycrystalline caused the concurrent dislocation glide during its irreversible transformation [5]. This condition of low recovery strain can not be implemented for engineering purposes. Manufacturing a single crystal structure is very difficult for massive production on the industrial scale. Several efforts were developed to improve the shape memory effect in polycrystalline of Fe-Mn-Si based, such as employing special heat treatment (thermomechanical treatment, training, and ausforming) [3], modification of chemical composition by adding the element that can form finer precipitation (Nb, C, V, etc.) [6] and stabilize the austenite phase (Mn and Ni) [7]. Fawkhry [4] concluded that the grain size of polycrystalline SMA has two conflicting effects during the phase transformation process. Small grains produced more  $\epsilon$ -martensite nucleation sites and more twin structures, which would hinder Shockley movement and lead to the deterioration of the SME. The more significant of twins showed the poor shape memory effect because the twins directly relate to low grain boundary energies that can't be restored by heating [8]. In contrast, Choi et al., [9] reported that the increase in grain size enhanced the volume fraction of thermally induced martensite due to the improving degree of recrystallization. The relations of variables and the effect of these studies need to be further investigated to improve performance for engineering purposes. Another study reported that thermomechanical treatment at ~600°C, particularly with rolling addition before the solution treatment, reduced the accumulated dislocation, improved the shape memory properties, developed a [111] texture in the austenite phase due to the increasing austenite stability in small grain [10]. Dynamic recrystallization activated during the rolling process at 1000 °C followed by annealing at 700 °C provides a more regularly shaped grain with low stacking fault than those by warm rolling (600 °C), further leading the improvement of SME in the Fe-17Mn-6Si-9Cr-5Ni-0.09C and Fe-22Mn-4Si-8Cr-5Ni [8].

Other than that, the high Mn levels in Fe-Mn-Si-based SMA usually range from 15 to 30%, which is a significant concern when this alloy is

to be massively produced. On the contrary, the lower Mn decreases the  $\epsilon$ -martensite stability and increases the martensite start transformation temperature. This problem was compensated for by adding the 4-5 wt.% Ni and 5-9 wt.% Cr, and large excess Si content [8]. So, applying thermomechanical treatment with appropriate chemical composition became critical in improving the shape memory effect.

In this work, the effect of pre-rolling before solution treatment with the varied temperature of each process was subjected to correlate its impact on the microstructure and mechanical properties of Fe-14Mn-4Si-8Ni-11Cr alloy.

## 2. MATERIALS AND METHODS

The Fe-Mn-Si-Ni-Cr alloy with the exact chemical composition, as shown in Table 1, was melted in an induction melting furnace. The  $Ni_{eq.}$  and  $Cr_{eq.}$  were calculated by the Hammer equation (Eq. 1-2) [11].

$$Cr_{eq} = Cr + 1.5Si + 1.37Mo + 2Nb + 3Ti \quad (1)$$

$$Ni_{eq} = Ni + 0.31Mn + 22C + 14.2N + Cu \quad (2)$$

The cast ingot was cut to 100 x 25 x 6 mm using a wire cut machine and then homogenized at 1050 °C for 3 hours. Two samples were rolled to around 3 mm of thickness (65% reduction) in three passes at 900 °C and two others at 1000 °C to determine the effect of hot rolling temperature.

Table 1. Chemical composition (wt.%) of Fe-Mn-Si-Cr-Ni alloy

Fe	Mn	Si	Cr	Ni	C
Balance	14.22	3.76	10.54	8.23	0.09

Then, each varied sample was performed on the solution treatment process at 1000 and 1100 °C for 30 minutes in an argon environment, followed by water quenching. The sample code is summarized in Table 2.

Table 2. Description of sample code

Sample Code	Description
A	As-cast
B	Hot rolling 900 °C and solution treatment at 1000 °C
C	Hot rolling 900 °C and solution treatment at 1100 °C
D	Hot rolling 1000 °C and solution treatment at 1000 °C
E	Hot rolling 1000 °C and solution treatment at 1100 °C

The shape memory behavior on the sample processed by thermomechanical was evaluated by the degree of tensile shape recovery (Eq. 3). Each

steel was prepared as a tensile sample with a gauge length of 25 mm and diameter of 6 mm, according to ASTM E8 standard. The pre-strain (10%) with 0.5 mm/min speed loaded was provided to give stress at room temperature, followed by unloading with the same speed using Tinius Olsen Hydraulic Universal Testing Machine. Finally, all specimens were heated at 600 °C for 15 minutes in Nabertherm Muffle Furnace with an argon environment to complete the reverse transformations for the recovery process. This method was introduced by Matsumura et al., [12].

$$SME = \frac{l_1 - l_2}{l_1 - l_0} \times 100\% \quad (3)$$

The  $l_0$ ,  $l_1$ , and  $l_2$  are the gauge lengths on the specimen before the tensile loading, after the unloading, and after the complete reverse transformation, respectively.

A metallographic test was carried out to confirm the microstructure using an optical microscope Olympus Type BX53M. Each sample was cut to 1x1 mm by a precision cutting machine, mounted in epoxy resin, mechanically ground using SiC paper (80-1200 grit), polished with alumina slurry (5 and 1  $\mu\text{m}$ ), and etched to Kalling etchant (made from 5 g  $\text{CuCl}_2$  + 100 mL HCl + 100 ml ethanol). The Heyn Lineal Intercept procedure (ASTM E112) calculated the grain size. The microstructure was also confirmed by XRD (x-ray diffraction) Bruker with Co-K $\alpha$  source (1.789 Å). Then, the Rietveld method was used to analyze its lattice parameter phase using GSAS-II. The hardness test was performed to investigate the change in hardness value using the AFRI Hardness tester machine with Brinell methods (diameter indenter of 5 mm).

### 3. RESULT AND DISCUSSION

#### 3.1 Microstructure analysis

Microstructure morphology before pre-strain, including the grain size of austenite and the annealing twins, feature, is crucial in determining the shape memory effect. Figure 1 shows the microstructure of Fe-14Mn-4Si-8Ni-11Cr as-cast and after thermomechanical treatment. In the ordinary optical microscope, the microstructure is a typical dendritic structure of the austenite phase. For the Fe-Mn-Si-Ni-Cr steels used in this study,  $C_{req}$ =16.18 wt.% and  $Ni_{eq}$ =14.62 wt.%, giving the ratio of Cr equivalent and Ni equivalent equal to 1.11, indicating the equilibrium solidification of Fe-Mn-Si-Ni-Cr follows the A modes ( $L \rightarrow$

$L+\gamma \rightarrow \gamma$ ) due to Mn that known as an austenite former during solidification [11].

After the thermomechanical process, the dendritic structure transformed into the fully austenitic structure with thermal twin (Figure 1b-e) and the finer slip line bands in particular grains, which were assumed to identify  $\epsilon$ -martensite after grinding. Slightly plastic deformation in compressive stress was induced by mechanical grinding or polishing with multiplicity orientation. A consequence due to low stacking faults energy of FeMnSi SMA and the external stress during grinding, the SIM (stress-induced martensite) transformation occurred, leading the  $\gamma$ -FCC grains to transform into  $\epsilon$ -martensite [13]. Its microstructure agrees with the report from other Fe-Mn-Si-Cr-Ni findings [10],[14]-[15]. Additionally, Fig. 1b shows the incomplete delineation grain boundary, possibly due to the misorientation variation [8]. Sample B exhibits a smaller grain size (29.43  $\mu\text{m}$ ) than Sample C (41.96  $\mu\text{m}$ ), suggesting that the higher solution treatment temperature provides more strain energy for completed recrystallization, migration of austenite grain boundaries, and growth during solution treatment [4][14]. With the higher temperature rolling, the grain size was increased to 42.44  $\mu\text{m}$  and 45.57  $\mu\text{m}$  for samples D and E, respectively. These values are higher than the sample that results in hot rolling of 900 °C, indicating the higher temperature in the rolling process increased thermal energy, which encouraged the atoms to move and form a new crystal structure [14].

Furthermore, the annealing twin with mostly straight boundary lines crossing the austenite grains is visible in sample B-E due to the lower stacking fault energy of Fe-14Mn-4Si-8Ni-11Cr during recrystallization. The annealing twin structure, as planar defects resulting in the stacking fault overlapped, was probably proposed as a growth accident, grain boundary dissociation, or the stacking fault package originates near the start of the migrating recrystallization and subsequently merged [15]-[16]. The average twin length is 90.97, 128.527, 135.23, and 160.88  $\mu\text{m}$  for samples B, C, D, and E, respectively. The twin spacing of the higher temperature sample (samples C and E) is larger than that of lower temperature (samples B and D). By increasing the temperature of hot rolling and solution treatment during plastic deformation, the number of twin and stacking faults reduces, representing the densities of annealing twin boundaries and grain boundaries decreases. Still, its length increases [15],[17]. The smaller grain size provides more site for the

formation of twins since it is driven by the stored energy consumption in the grain boundary [16].

The XRD also confirms these microstructures, as shown in Fig. 2. According to the Schaeffler diagram, Fe-14Mn-4Si-8Ni-11Cr only contains a

full austenite phase; however, XRD results indicate the presence of dominated  $\gamma$ -FCC and relatively weak intensity of  $\epsilon$ -HCP (metastable phase) as impurities peak.

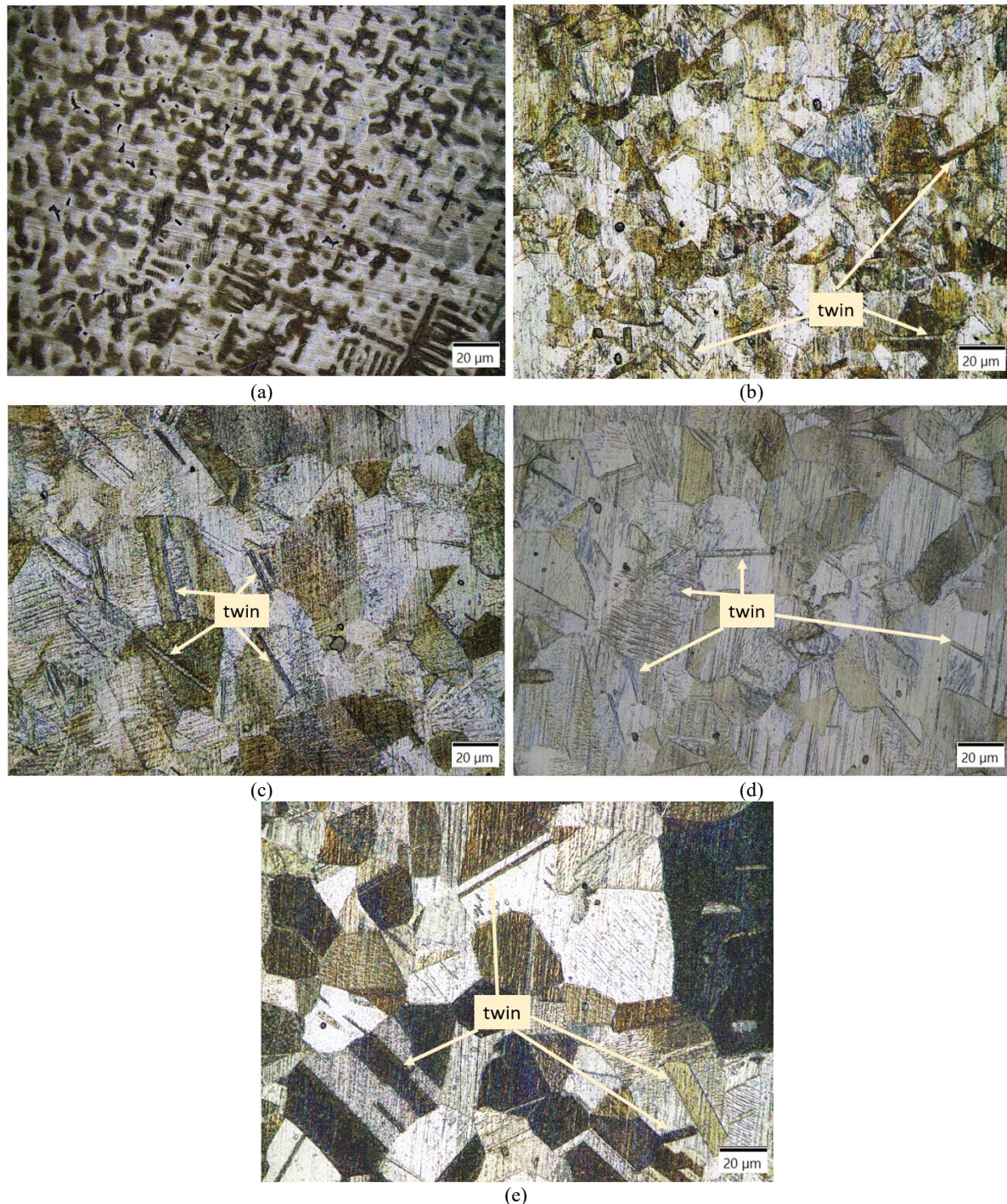


Figure 1. Microstructure of Fe-14Mn-4Si-8Ni-11Cr (a) sample A (as-cast), with hot rolling 900 °C, (b) sample B (solution treatment 1000 °C), (c) sample C ( solution treatment 1100 °C), and hot rolling 1000 °C (d) sample D (solution treatment 1000 °C), and (e) sample E (solution treatment 1100 °C). Etched by Kalling's

The  $\gamma$  -FCC parent phase is depicted in the planes of (111), (200), (220), (311), and (222), which is identical to prior research [14]. The formation of  $\epsilon$ -HCP in a small fraction (2.66-6.3%) was assisted by mechanical ground and the

shifted temperature transformation (thermal-induced), according to the Clausius-Clapeyron [10]. There is no significant relationship between rolled or solution temperature and  $\epsilon$ -HCP fraction

(Table 3). The higher  $\epsilon$ -HCP fraction (6.3%) was obtained by sample D.

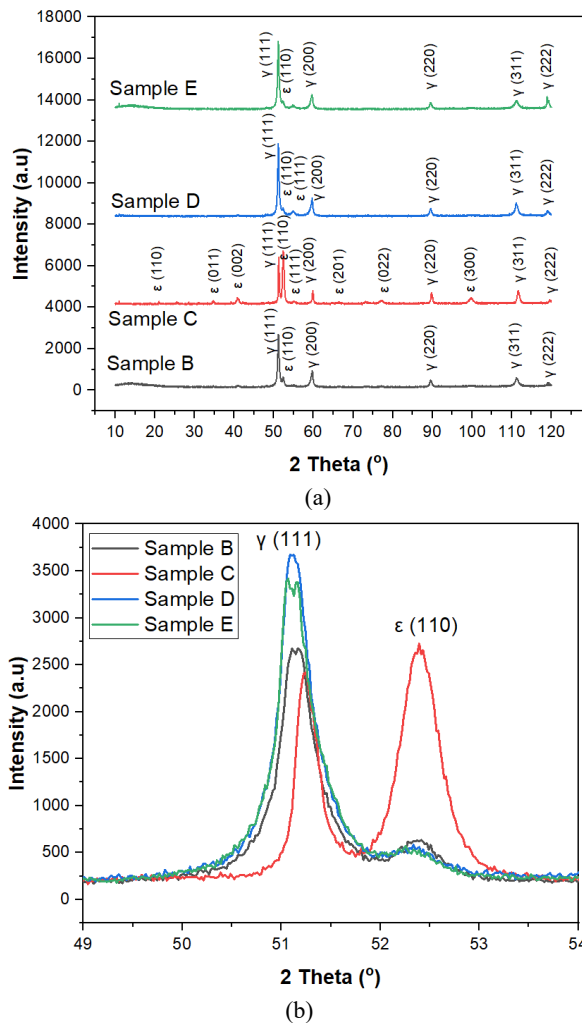


Figure 2. XRD pattern of (a) Fe-14Mn-4Si-8Ni-11Cr and (b) inserted at 49°-54° of 2 $\theta$

Figure 2(b) shows that the reflection peak in 2 $\theta$  of 51.08° and 52.37° indicated the twin appearance, referring to two symmetric structures in the same layer stuck together in the primary structure (111  $\gamma$ -phase) [18]. The twin structure reduced the elastic deformation resistance [19]. It is consistent with the microstructure result (Fig. 1). In addition, the lattice parameter of each phase is summarized in Table 3. Lattice a in  $\gamma$ -cell (space group Fm – 3m) is shifted and tend to broaden as the temperature increase, except in sample C. If the lattice parameter is broader, the crystal structure may be less dense, making the material less resistant to mechanical stress [20], and martensitic transformation can quickly occur [19].

### 3.2 Hardness Analysis

The effect of hot rolling and solution treatment process on Fe-14Mn-4Si-8Ni-11Cr is shown in Fig. 3. The Fe-Mn-Si-Ni-Cr as-cast had

the lowest hardness value (175.72 BHN), while sample B had the maximum value (315.48 BHN). The random direction of the dendritic structure most likely caused the low hardness of the as-cast austenitic structure.

Table 3. Lattice parameters of diffraction pattern in Fe-14Mn-4Si-8Ni-11Cr

Parameter	Sample			
	B	C	D	E
<b><math>\gamma</math>-FCC (cubic)</b>				
Space group: Fm – 3m				
Lattice a (nm)	3.59323	3.58506	3.59513	3.59561
Phase fraction	96.24%	93.52%	93.7%	97.34%
<b>E-HCP (hexagonal)</b>				
Space group: P- 3m1				
Lattice a (nm)	4.04652	4.052	4.052	4.0469
Lattice c (nm)	5.09976	5.085	5.085	5.13585
Phase fraction	3.76%	5.648%	6.3%	2.66%
Rwp (%)	3.01	4.4	4.28	4.25
Chi square	1.73	1.970	1.829	1.806

The thermomechanical addition generally improved the hardness value compared to the as-cast sample. Hardness increases are inversely related to the grain size. According to the Hall-Petch equation, the harder the material, the smaller the grain size.

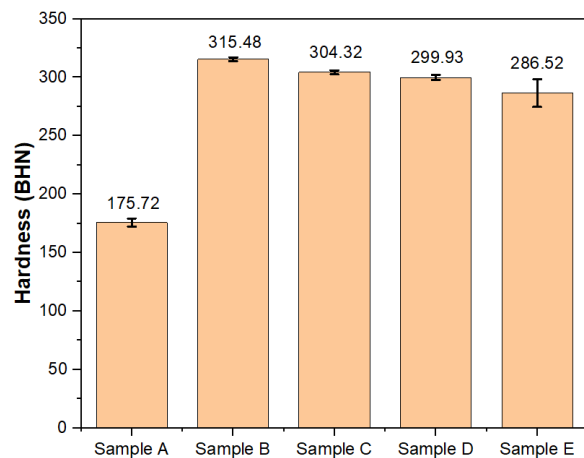


Figure 3. Hardness result of Fe-14Mn-4Si-8Ni-11Cr after hot rolling and solution treatment

The higher temperature in the rolling and solution treatment process provided more activation energy for completing recrystallization and consuming the deformed austenite and its twins, decreasing grain boundary and indirectly lowering hardness [16]. The existence of twins also contributed to the insignificant decrement of hardness in sample C (304.32 BHN) and sample E (286.52 BHN), which increased the work

hardening rate and disturbed dislocation mobility by creating barriers to dislocation glide [21].

### 3.3 Shape Memory Effect Analysis

The 10% pre-strain and recovery annealing temperature at 600 °C were used to determine the SME (in terms of the tensile recovery ratio) based on the microstructure data described above. The SME in Fe-Mn-Si-Ni-Cr shape memory alloys (Fe-SMAs) is derived on the stress-induced  $\epsilon$ -martensite transformation ( $\gamma(\text{FCC}) \rightarrow \epsilon(\text{HCP})$ ) at room temperature and the reverse transformation ( $\epsilon \rightarrow \gamma$ ) by heating at higher temperature [1]. The effect of thermomechanical conditions on the SME is shown in Fig. 4.

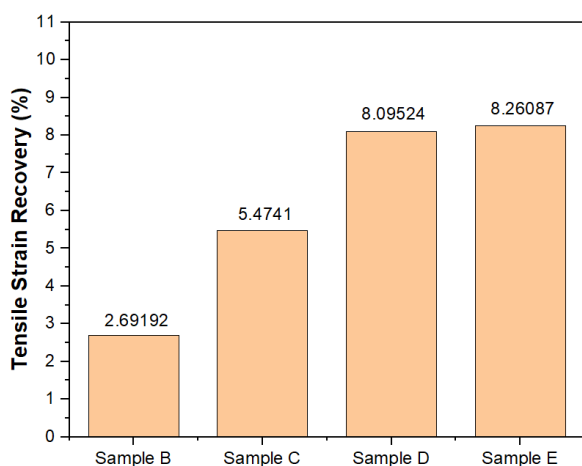


Figure 4. Tensile strain recovery ratio of Fe-14Mn-4Si-8Ni-11Cr

Based on Fig. 4, the tensile recovery ratio of Fe-14Mn-4Si-8Ni-11Cr after annealing at 600°C is 2.69%, 5.47%, 8.09%, and 8.26% for samples B, C, D, and E, respectively. Compared to other Fe-Mn-Si-Ni-Cr alloys, Fe-14Mn-4Si-8Ni-11Cr shows a relatively good shape memory effect (Table 4). Sample E has the largest recovery strain, around 8.26%, while sample B has the poorest SME (2.69%). The number of SMEs is correlated to the amount of stacking faults, grain size, and the twin's morphology [9]. The larger grain size provided more the atomic arrangement of stacking fault in the FCC austenite during pre-straining can act as a nucleus site for the  $\epsilon$ -martensite preferentially nucleated and growth, affecting the improvement of shape memory [9],[14],[22]. The higher temperature in solution treatment significantly promotes the martensite start temperature close to the ambient temperature, generating a high amount of martensite. Choi et al., concluded that the volume fraction of thermally induced  $\epsilon$ -martensite after solution treatment increased with the increasing

temperature, caused by the reduction of dislocation density along with the increasing grain size, the decreasing critical stress for stress-induced martensite transformation ( $\sigma_{\text{SIM}}$ ) and the completing recrystallization degree [9].

Table 4. Comparison of SME result of Fe-Mn-Si-Ni-Cr shape memory alloy

Materials	SME	Remark	Ref.
e-14Mn-4Si-8Ni-11Cr	2.69 %	As hot rolled (900 - 1000 °C) + solution treated (1000 - 1100 °C for 30 minutes)	This study
Fe-21.63Mn-5.6Si-9.32Cr-5.38Ni	4.5 % - 5.5 %	Cold rolling + annealing (1100 - 1150 °C for 5-120 minutes)	[15]
Fe-18.54Mn-5.70Si-8.91Cr-4.45Ni	2.7 % - 7.7 %	As-cast, as-annealed (300 - 1100 °C for 30 minutes)	[22]

Furthermore, the highest SME in sample E was caused by the lower number of annealing twins, which can't revert through heating in the recovery process [15]. On the other hand, the pre-existing  $\epsilon$ -martensite (Figs.1(b)-1(e)) inhibits the martensite transformation generated by pre-strain because its band intersection acts as a significant barrier to partial dislocation movement.

## 4. CONCLUSION

The shape memory effect characteristics of Fe-14Mn-4Si-8Ni-11Cr were improved through thermomechanical processing for seismic applications. The austenite became larger as the hot rolling and solution treatment temperature increased, suggesting that recrystallization had been completed and grain growth had occurred for the rolled grain. Because of the lower stacking fault energy and other lead provided the stored energy consumption in the grain boundary, the number of annealing twins increased, the twin spacing became narrower, and the average twin length decreased from 160.88  $\mu\text{m}$  to 90.97  $\mu\text{m}$  at lower rolling and solution treatment temperatures. Furthermore, thermomechanical addition improved the hardness value (286.52-315.48 BHN) compared to the as-cast sample (175.72 BHN). Increasing the hot rolling and solution treatment temperature was found to reduce hardness slightly but noticeably increased the tensile recovery ratio of Fe-14Mn-4Si-8Ni-11Cr. It seemed inversely related to the austenitic grain size, revealing that twin formation as tangles barrier caused the increase in work hardening and disturbed dislocation mobility to gliding. Controlling the grain size of the austenitic phase (29.43-45.57 $\mu\text{m}$ ) and the pre-existence of  $\epsilon$ -

martensite throughout the thermomechanical process resulted in recovery strains varying from 2.69% to 8.26%. The highest-performing SME with an 8.26% tensile recovery ratio was found to be Fe-14Mn-4Si-8Ni-11Cr with the hot rolling and solution treatment at 1100 °C temperature.

## ACKNOWLEDGMENT

The authors would like to thank financial support from the Research Organization of Nanotechnology and Materials (ORN-M-BRIN). This research was conducted using the facilities and technical support at the Research Center for Metallurgy, National Research and Innovation Agency (BRIN).

## REFERENCES

- [1] J. Mohd Jani, M. Leary, A. Subic, and M. A. Gibson, "A review of shape memory alloy research, applications and opportunities," *Mater. Des.*, vol. 56, no. April, pp. 1078-1113, 2014. Doi: 10.1016/j.matdes.2013.11.084.
- [2] A. Tabrizikahou, M. Kuczma, M. L. Plura, E. N. Pursangi, M. Noori, P. Gardoni and S. Li, "Application and modelling of shape-memory alloys for structural vibration control: State-of-the-art review," *Constr. Build. Mater.*, vol. 342, no. PB, pp. 127975, 2022. Doi: 10.1016/j.conbuildmat.2022.127975.
- [3] H. Peng, J. Chen, Y. Wang, and Y. Wen, "Key factors achieving large recovery strains in polycrystalline Fe-Mn-Si-based shape memory alloys: A review," *Adv. Eng. Mater.*, vol. 20, no. 3, pp. 1-18, 2018. Doi: 10.1002/adem.201700741.
- [4] M. K. El Fawkhry, "The effect of solution treatment temperature on SIEM and shape recovery of Fe-Mn-Si shape memory alloy," *J. Mater. Res. Technol.*, vol. 15, pp. 1069-1075, 2021. Doi: 10.1016/j.jmrt.2021.08.009.
- [5] X. Min, T. Sawaguchi, X. Zhang, and K. Tsuzaki, "Reasons for incomplete shape recovery in polycrystalline Fe-Mn-Si shape memory alloys," *Scr. Mater.*, vol. 67, no. 1, pp. 37-40, 2012. Doi: 10.1016/j.scriptamat.2012.03.015.
- [6] Y. Yang, C. Leinenbach, and M. Shahverdi, "Simulation and experimental characterization of VC precipitation and recovery stress formation in an FeMnSi-based shape memory alloy," *J. Alloys Compd.*, vol. 940, pp. 168856, 2023. Doi: 10.1016/j.jallcom.2023.168856.
- [7] C. Zhang, F. Song, S. Wang, H. Peng, and Y. Wen, "Effect mechanism of Mn contents on shape memory of Fe-Mn-Si-Cr-Ni alloys," *Jinshu Xuebao/Acta Metall. Sin.*, vol. 51, no. 2, pp. 201-208, 2015. Doi: 10.11900/0412.1961.2014.00394.
- [8] I. Esquivel, M. F. Giordana, and A. V. Druker, "Effect of heat treatment on the microstructure and shape memory behaviour of Fe-Mn-Si-Ni-Cr alloys," *Mater. Charact.*, vol. 155, pp. 109811, 2019. Doi: 10.1016/j.matchar.2019.109811.
- [9] S. Choi, E. Choi, and W. J. Kim, "Austenite grain size effect on recovery stress and recovery strain of Fe-Mn-Si-Cr-Ni-0.01C alloy severely plastically deformed by differential speed rolling," *Mater. Charact.*, vol. 175, pp. 111097, 2021. Doi: 10.1016/j.matchar.2021.111097.
- [10] M. Mohri, I. Ferretto, C. Leinenbach, D. Kim, D. G. Lignos, and E. Ghafoori, "Effect of thermomechanical treatment and microstructure on pseudo-elastic behavior of Fe-Mn-Si-Cr-Ni-(V, C) shape memory alloy," *Mater. Sci. Eng. A*, vol. 855, pp. 143917, 2022. Doi: 10.1016/j.msea.2022.143917.
- [11] H. Peng, Y. Wen, Y. Du, Q. Yu, and Q. Yang, "Effect of manganese on microstructures and solidification modes of cast Fe-Mn-Si-Cr-Ni shape memory alloys," *Metall. Mater. Trans. B Process Metall. Mater. Process. Sci.*, vol. 44, no. 5, pp. 1137-1143, 2013. Doi: 10.1007/s11663-013-9880-2.
- [12] O. Matsumura, T. Sumi, N. Tamura, K. Sakao, T. Furukawa, and H. Otsuka, "Pseudoelasticity in an Fe-28Mn-6Si-5Cr shape memory alloy," *Mater. Sci. Eng. A*, vol. 279, no. 1-2, pp. 201-206, 2000. Doi: 10.1016/s0921-5093(99)00644-9.
- [13] S. Y. Jiang, Y. Wang, X. D. Xing, and Y. Q. Zhang, "Stress-induced martensite phase transformation of FeMnSiCrNi shape memory alloy subjected to mechanical vibrating polishing," *Trans. Nonferrous Met. Soc. China (English Ed.)*, vol. 30, no. 6, pp. 1582-1593, 2020. Doi: 10.1016/S1003-6326(20)65321-3.
- [14] M. M. Pan, X. M. Zhang, D. Zhou, R. D. K. Misra, and P. Chen, "Fe-Mn-Si-Cr-Ni based shape memory alloy: Thermal and stress-induced martensite," *Mater. Sci. Eng. A*, vol. 797, pp. 140107, 2020. Doi: 10.1016/j.msea.2020.140107.
- [15] L. Yong, Q. Luo, H. Peng, J. Yan, B. Xu,

- and Y. Wen, “Dependence of shape memory effect on austenitic grain sizes in thermo-mechanical treated Fe-Mn-Si-Cr-Ni shape memory alloys,” *Mater. Charact.*, vol. 169, pp. 110650, 2020. Doi: 10.1016/j.matchar.2020.110650.
- [16] N. Bozzolo and M. Bernacki, “Viewpoint on the formation and evolution of annealing twins during thermomechanical processing of FCC metals and alloys,” *Metall. Mater. Trans. A Phys. Metall. Mater. Sci.*, vol. 51, no. 6, pp. 2665-2684, 2020. Doi: 10.1007/s11661-020-05772-7.
- [17] K. W. Park, E. Choi, and W. J. Kim, “Grain size effect on the recovery stress and strain of a Fe–Mn–Si shape memory alloy in a wide range of grain sizes,” *Mater. Sci. Eng. A*, vol. 856, pp. 143947, 2022. Doi: 10.1016/j.msea.2022.143947.
- [18] Y. Chen, A. Li, Z. Ma, G. Kang, D. Jiang, K. Zhao, Y. Ren, L. Cui, K. Yu, “Revealing the mode and strain of reversible twinning in B19' martensite by in situ synchrotron x-ray diffraction,” *Acta Mater.*, vol. 236, p. 118131, 2022. Doi: 10.1016/j.actamat.2022.118131.
- [19] P. Chowdhury, “Frontiers of theoretical research on shape memory alloys: A general overview,” *Shape Mem. Superelasticity*, vol. 4, no. 1, pp. 26-40, 2018. Doi: 10.1007/s40830-018-0161-4.
- [20] L. La Rosa and F. Maresca, “On the impact of lattice parameter accuracy of atomistic simulations on the microstructure of Ni-Ti shape memory alloys,” *Model. Simul. Mater. Sci. Eng.*, vol. 30, no. 1, 2022. Doi: 10.1088/1361-651X/ac3b9e.
- [21] K. Renard and P. J. Jacques, “On the relationship between work hardening and twinning rate in TWIP steels,” *Mater. Sci. Eng. A*, vol. 542, pp. 8-14, 2012. Doi: 10.1016/j.msea.2012.01.123.
- [22] H. Peng, L. Yong, S. Wang, and Y. Wen, “Role of annealing in improving shape memory effect of as-cast Fe-Mn-Si-Cr-Ni shape memory alloys,” *Metall. Mater. Trans. A Phys. Metall. Mater. Sci.*, vol. 50, no. 7, pp. 3070-3079, 2019. Doi: 10.1007/s11661-019-05233-w.